2019

Rotary Friction Welding Versus Fusion Butt Welding of Plastic Pipes – Feasibility and Energy Perspective

Ramsey F. Hamade
American University of Beirut, Lebanon

Tarek R. Andari
American University of Beirut, Lebanon

Ali H. Ammouri
Lebanese American University, Lebanon

Ibrahim S. Jawahir
University of Kentucky, is.jawahir@uky.edu

Repository Citation

Available online at www.sciencedirect.com

ScienceDirect

Procedia Manufacturing 33 (2019) 693–700

Procedia MANUFACTURING

www.elsevier.com/locate/procedia

16th Global Conference on Sustainable Manufacturing - Sustainable Manufacturing for Global Circular Economy

Rotary Friction Welding versus Fusion Butt Welding of Plastic Pipes – Feasibility and Energy Perspective

Ramsey F. Hamade[a], Tarek R. Andari[a], Ali H. Ammouri[b], I.S. Jawahir[c]

[a]*Department of Mechanical Engineering, American University of Beirut, Beirut, Lebanon*
[b]*Department of Industrial and Mechanical Engineering, Lebanese American University, Byblos, Lebanon*
[c]*Department of Mechanical Engineering, University of Kentucky, UK Center for Manufacturing , Lexington, Kentucky 40506-0108*

Abstract

According to the Plastics Pipe Institute, butt fusion is the most widely used method for joining lengths of PE pipe and pipe to PE fittings "by heat fusion" (https://plasticpipe.org/pdf/chapter09.pdf). However, butt-welding is not energy-cognizant from the point of view of a phase-change fabrication method. This is because the source of heating is external (heater plate). The initial heating and subsequent maintenance at relatively high temperature (above 200 C for welding of high-density polyethylene pipe) is energy intensive. Rotary friction welding, on the other hand focuses the energy where and when as needed because it uses electric motor to generate mechanical (spinning) motion that is converted to heat. This work will make the case for friction heating as energy efficient. An initial feasibility study will also be introduced to demonstrate that the resulting welded pipe joints may be of comparable quality to those produced by butt fusion and to virgin PE material.

Selection and peer-review under responsibility of the scientific committee of the 16th Global Conference on Sustainable Manufacturing (GCSM).

Keywords: Rotary Friction Welding; Energy Consumption; Fusion Butt Welding

1. INTRODCUTION

Strict emission laws and organizations such as the European Emission Standards and ACARE (flight global) 2050 are leading the world towards cleaner and greener energy. The efforts push industry leaders to produce material alternatives and reduce the environmental impact from manufacturing operations [1, 2]. Thus, shifting operations towards leaner and energy efficient manufacturing is of great importance.

Polyethylene (PE) has superior corrosion and chemical resistance, excellent insulation properties, it is lightweight and flexible, and the cost of manufacturing is relatively low [3]. Material properties are presented in Table 1.

Selection and peer-review under responsibility of the scientific committee of the 16th Global Conference on Sustainable Manufacturing (GCSM).
10.1016/j.promfg.2019.04.087

Table 1: Geometric and Material Properties of HDPE 100 [4]

Property	Density (g/cm^3)	Yield Stress (MPa)	Elongation (%)	Melt flow index	Diameter, D (m)	Thickness, d (m)	Length, L (m)
	0.952	26.2	>= 350	0.48	0.063	0.0058	0.200

In addition, rotary friction welding (RFW) offers a range of significant advantages that include, an environmental friendly process with short cycle times that can be used to join similar and dissimilar materials. RFW is a steady – state frictional process developed during the Second World War. It is used for joining parts with rotationally symmetrical surfaces. Frictional welding processes convert mechanical energy into heat at the joint to be welded. The parts are rubbed together at the joining interface under axial pressure (normal to plane surfaces) and unidirectional circular motion. This results in frictional heating that melts the material in the joining zone. When the circular motion is stopped, the molten material solidifies under pressure, forming a weld [5, 6].

Much has been reported on appropriate RFW input parameter selection for high PE joint quality. However, little effort has been placed on reporting the energy consumption of producing welds with these parameters [6-10]. In their useful study of friction welding, the authors showed that active control of the resulting grain size and distribution is critical in achieving the desired joint strength. Active control was carried out by real-time control of the process input variables (such as speed, force, torque-control schemes). In return, this allowed for control over the relevant state variables (e.g., temperature and bead size). Excellent control results have been achieved and provide solid foundations for correlating the energy consumption with selected input process parameters [10].

2. RFW PROCESS AND SEQUENCE PHASES

The RFW process is categorized into four distinct phases (Phases A, B, C, D) in Figure 1(a) represented in terms of axial displacement and temperature versus time phases (Phases I, II, III, IV), respectively in Figure 1(b). The main process parameters for spin welding are, the weld velocity, RPM, the weld pressure, (P1, P2), and the weld time (t1, t2). One part is rigidly clamped while the other is rotated to the desired speed. At time t1, the parts are brought into contact by means of axial pressure, P1. Abrasion will first strip off the surface roughness, then parts will have full surface contact. This phase is termed 'Solid material-friction', where the heat generated by Coulomb friction results in a temperature increase in plastic, Phase I in Figure 1(b). Melting begins during the 'Unsteady-state friction' phase (Phase II) once the temperature reaches the crystalline melting point of the material or glass transition temperature. The pressure P1 causes a laterally outward flow of the molten film, which in turn results in an increase of axial displacement with time. This is followed by the 'Steady-state friction' phase (Phase III), in which the rate of melting equals the rate of outflow, leading to a linearly increasing axial displacement with time. The molten film continues to flow while cooling, which results in further increase in axial displacement (Phase IV) [7-8].

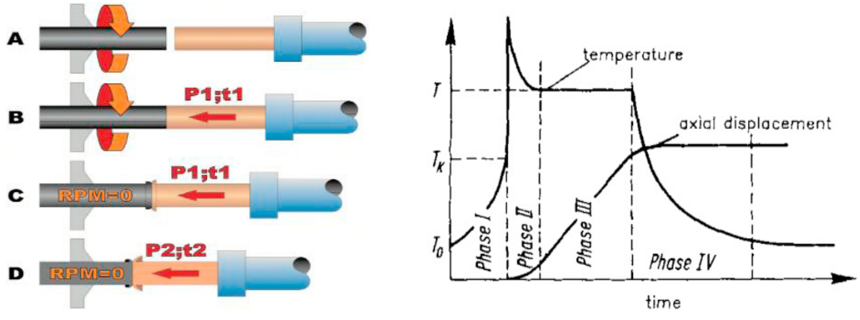

(a) (b)

Figure 1: a) RFW processs [9] b) axial displacement vs time and temperature vs time [8].

3. FUSION BUTT WELDING HEAT CONSUMPTION ANALYSIS

Fusion butt welding may be classed as a heat transfer model comprising of three phases, i) heating from room temperature, ii) steady state convection, as well as iii) conduction. The convective states correspond to heating the plate from room temperature and maintaining the heat for any given time. Conductive heat transfer resembles the contact between the heated tool and pipes, where the heat transfer coefficient of polyethylene is 0.46 [11]. Heat transfer with the environment is accounted for using a convective heat coefficient of 20 W/m^2(ºC) at a constant temperature of 20 ºC [9]. In their useful study of fusion butt welding, the authors proposed optimum parameters for welding HDPE, their reported heating and complete welding cycle times were 75s and 255s respectively [12]. For comparison, a conventional aluminium plate without Teflon coating is assumed. The TP 125 product specifications provided by [13], are utilised in the calculations below. As stated, the mass of the plate is 2.13 Kg and the time to reach welding temperature is approx. 10 minutes. The plate is heated from room temperature (293K) to the required melting temperature of T_m HDPE= 493 K. The length of pipe is 105mm and is assumed to be at room temperature. Using Equations 1-4, the total power consumption of heating a PE is obtained and presented in Table 2.

Phase I (Specific Heat Equation):

$$H = m * C_p * \Delta T \quad (1)$$

Where,
H (kJ) = Energy
$m\ (Kg)$ = Mass
$C_p\ (Specific\ heat\ of\ Alumium) = 0.91 \frac{kJ}{Kg * K}$
$T\ (K)$ = Temperature

A conversion constant is used to obtain the power consumption.

$$P = H * 2.8e^{-4} \quad (2)$$

Where,
$P\ (kWh)$ = Power Consumption

Using Newton's Law of Cooling [14],
Phase II (Steady-State Convection):

$$Q = \left(h_{air} * A_{plate} * \Delta T\right) * t \quad (3)$$

Where,
$Q\ (Wh)$ = Convection Energy
$h_{air}\ (\frac{W}{m^2 * °C})$= Convective heat coefficient
$A_{plate}\ (m^2) = 2 * \pi * (r^2)$
ΔT (°C) = $T_{plate} - T_{air}$
$t\ (h)$ = time

Phase III (Conduction):

$$Q = \frac{(k_{PE} * A_{pipe} * \Delta T)}{\Delta x} * t \quad (4)$$

$Q\ (Wh)$ = Conduction Energy
$k_{PE}(Wh) = 0.28$

$A_{pipe}\ (m^2) = \pi * (\frac{D^2}{4})$
$\Delta T\ (°C) = T_{plate} - T_{pipe}$
$\Delta x\ (m)$ =Length of pipe

Table 2: Fusion Butt Welding Power Consumption

	Phase I	Phase II	Phase III	Total
Power Consumption (Wh)	109	19	0.04	128.04

4. PROCESS PARAMETERS

Welding parameters greatly influence the final weld quality; thus, an appropriate selection of parameters is critical in achieving the desired weld strength. [7] and [8] carefully analysed the effect of speed of rotation, axial pressure, interfacial torque and axial displacement on the final weld quality. The authors displayed that a weld factor of 1 for HDPE was achievable at tangential speed (v_t) equal to 3.6 m/s and axial velocity close to 0.5 mm/s (red highlights Figures 2 (a) and (b). Weld strength is represented as weld factor (f), which can be obtained using equation (5) [7]:

$$f = \frac{yield\ stress\ of\ welded\ material}{yield\ stress\ of\ non\text{-}welded\ material} \quad (5)$$

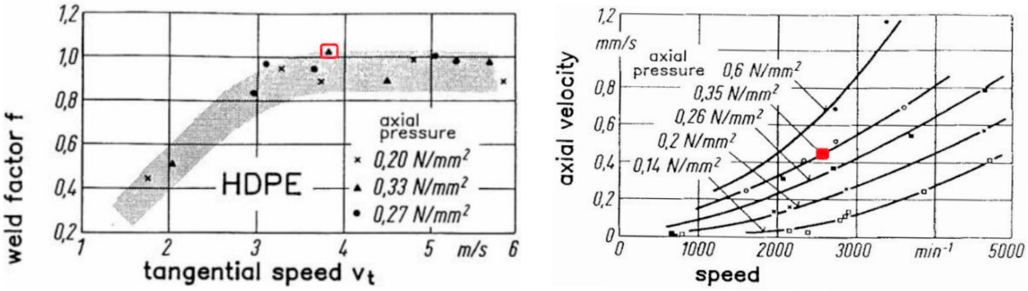

(a) (b)

Figure 2[8]: (a) weld factor vs tangential speed (b) axial velocity vs axial pressure

From the study [8], simplifying assumptions were used for the analysis. As shown in Figure 3 is a simple part geometry as assumed for the pipe cross section that entails an annular contact surface whose diameter is greater than the wall thickness. Weld strength is represented as weld factor (f), which can be obtained using equation (2) [7]. The data obtained from literature were utilized to develop the test matrix displayed in Table 3. The feed depth was constant at 10mm for all test cases. The tool rotational speed was varied from 1224 RPM to 1884 RPM, the feed rate from 20 mm/min to 60 mm/min. Displayed below each cell is the ratio of RPM to feed rate.

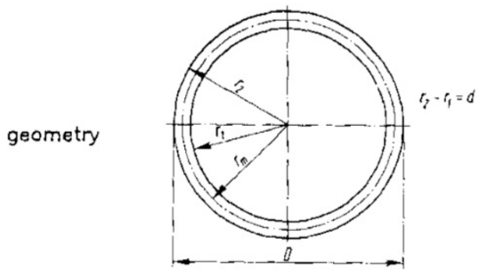

Figure 3: Simple part geometry (pipe cross-section) [8]

From Figure 3, the wall thickness (d) is found by subtracting the inner radius (r1) from (r2). Hence, the tangential velocity (v_t) is obtained using equation (6):

$$v_t = \pi \eta_0 (D - d) \quad (6)$$

Where,

$v_{t\,(\frac{m}{min})}$ = Tangential velocity

$\eta_0 (\frac{1}{min})$ = RPM

$D\ (m)$ = Diameter

$d\ (m)$ = Thickness

Table 3: Experimental test matrix with RPM to feed rate ratio

		Feed rate (mm/min)				
		20	30	40	50	60
RPM	1224	**(A1) 61.2**	**(A2) 40.8**	**(A3) 30.6**	**(A4) 24.48**	(A5) 20.4
	1554	**(B1) 77.7**	**(B2) 51.8**	**(B3) 38.85**	**(B4) 31.08**	(B5) 25.9
	1884	(C1) 94.2	**(C2) 62.8**	**(C3) 47.1**	(C4) 37.68	(C5) 31.4

5. EXPERIMENTAL

RFW was performed on the HAAS VF6 vertical machining center, which was installed with external hardware. Firstly, a work piece fixture (Fig. 2(a)) was designed to firmly mount the top half of the pipe onto the spindle head and the bottom half onto the CNC bed using a KURT vice (Fig. 2(b)). A Kistler Rotary 4-Component (Fx, Fy, Fz, and Torque (τ) Dynamometer (Type 9123C) was also attached to the spindle head (Fig. 2(b)). The Kistler 5223 B charge amplifier acquires and amplifies the signal emanating from the dynamometer, which is then collected by a custom LabView software. K-Type thermocouples were utilized in order to collect temperature profiles. In addition, hall-effect transducers were tapped directly to each phase line (spindle motor and z-drive motor). This allowed for raw voltage data acquisition that would be calibrated to obtain the motor current reading. Data of each welding operation is stored in a technical data management storage (TDMS) format that is easily accessible and requires little disk cost for data storage. More information on the set-up can be found in [10].

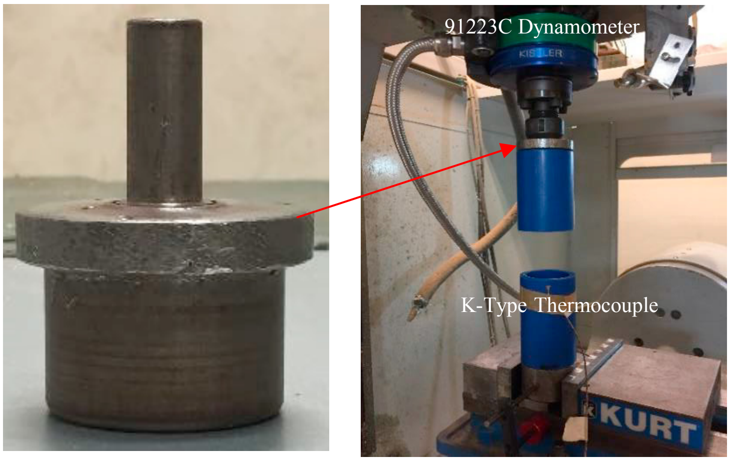

(a) (b)

Figure 4: (a) Fabricated workpiece fixture (b) Pipe mounted to the dynamometer

6. RESULTS

Photographs of three select test cases joined at room temperature are presented in Figure 5. Visual inspections indicated that the weld bead sizes were greater for lower feed rates (Figures 5(a,c)). Color change was apparent at higher RPM (see Fig. 5(c)) which may be a result of higher temperature in the heat-affected zone. Figure 5 (b) shows some correlation between weld quality and their corresponding input parameter selection, a weld bead of negligible size can be seen for both.

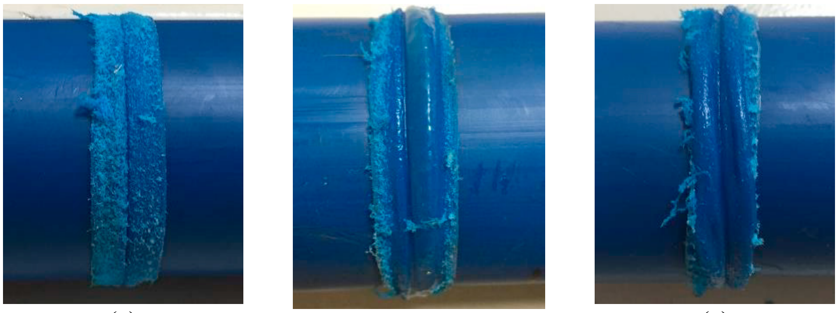

(a) (b) (c)

Figure 5: RFW samples at room temperature; (a) A3 (b) B3 (c) C3

Thrust forces (Fz) and torques collected from the dynamometer were used to calculate the axial pressures and power consumptions for each test case. Two methods were used to calculate the power consumptions. Method 1) a conversion from mechanical work to electrical work using Equation 8. Method 2) Torques (τ) were compared to previously obtained data in order to determine the spindle motor currents, which were used in a three-phase AC motor line to ground equation. The authors noted that the relationship between the torque and current was 1 Nm/Amp [10]. Using the thrust forces obtained from Figure 6 in Equation 7, axial pressures were calculated. The current profile and torques obtained from Figure 7 in Equations 8 and 9 were used to calculate power consumptions. A cost comparison between the power consumptions obtained from method 2 and fusion butt welding is presented for selected values in Table 4. The price of 1 kWh in Lebanon is used, this amounts to \$0.1. The depth of 10mm was achieved quicker for test cases with higher RPM and required less thrust force and torque, this is due to the achievement of the melting temperature quicker. Selected temperature profiles are presented in Figure 8.

$$Pr = F_z/S \tag{7}$$

Where,
$\mathrm{Pr}(N/mm^2)$ = Axial Pressure
$F_z\ (N)$ = Force in Z-direction
$S\ (mm^2)$ = Area of Pipe

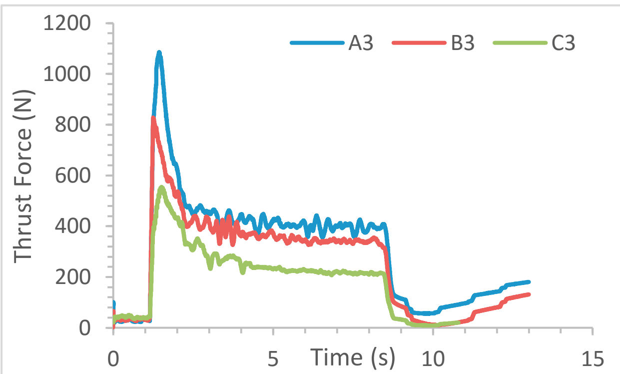

Figure 6: Experimental thrust forces for test cases A3, B3, C3

Method 1:

$$P = (\tau * \omega * t)/1000 \quad (8)$$

Where,
$P\ (kWh)$ = Power
$\tau\ (Nm)$ = Torque
$\omega\ \left(\frac{rad}{s}\right)$ = Angular Velocity

Method 2:

$$P = (3 * PF * I * V_{L-N} * t)/1000 \quad (9)$$

Where,
$P\ (kWh)$ = Power
PF = Power Factor of motor
$I\ (Amps)$ = Current
$V_{L-N}\ (Volts)$ = Line to Neutral Voltage

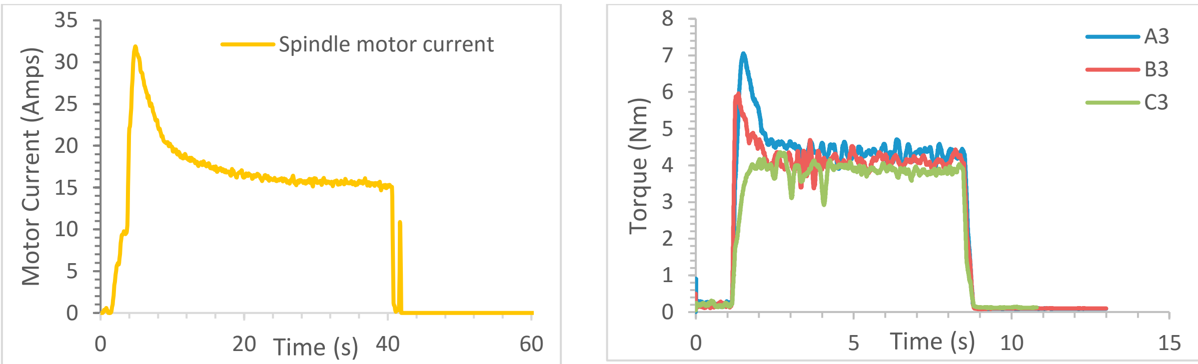

(a) (b)

Figure 7: (a) Net RMS spindle current [10] (b) Experimental torques for test cases A3, B3, C3

Test case A3 at rotational speed of 1224 RPM and feed rate 40, experienced a maximum thrust force of approximately 1085 N at a maximum torque of around 7 Nm, which required a maximum current of 7 Amps. The maximum temperature achieved was about 250ºC, well above the melting temperature required. This was achieved in 8.5 seconds and proves that RFW requires shorter cycle times than fusion butt welding. The thrust force and torque reach a maximum before decreasing to a constant steady-state phase.

Table 4: Axial Pressures and Power Consumption comparison between Fusion Butt Welding and RFW

	Fusion Butt Welding	A3	B3	C3
$Pr(N/mm^2)$	-	0.35	0.27	0.18
$P\ (kWh)$: Method 1	**From Table 2:**	0.0033	0.0035	0.0026
$P\ (kWh)$: Method 2	**0.128**	0.017	0.013	0.008
Cost ($)	0.0128	0.0017	0.0013	0.0008

It can be seen that higher temperatures were achieved at higher RPM, this provides a great indication for further study on the effect of input parameters on heat generation to produce high quality welds. The cycle time achieved with input parameters of C3 was 12s compared to that of 13.5s for A3 and B3. This is due to quicker material softening from increased temperature, thus a feed depth of 10mm is completed quicker.

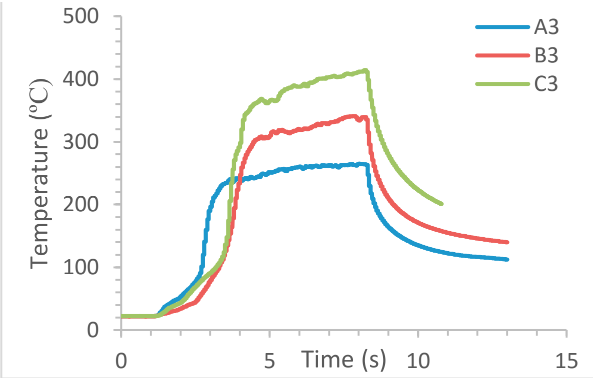

Figure 8: Experimental temperatures for test cases A3, B3, C3

7. CONCLUSION

Presented in this paper is a feasibility and energy study between the conventional method for joining HDPE pipes (Fusion Butt Welding) and rotary friction welding. Fusion butt welding is classed as a heat transfer model involving three phases, i) heating from room temperature, ii) steady state convection (maintaining the heat for any given period) and iii) conduction (contact between pipes and heating plate). The total of the energy consumption of each of the phases is determined using a popular welding machine specification. Active control is carried out by real-time control on the process input variables, this allowed for data acquisition of thrust forces, torques and temperatures. Temperature profiles showed that the meting temperature is achieved in under 10 seconds and indicates that further analysis on heat generation is required to better understand the effect of the process input parameters on the weld quality. Experimental measurements of thrust forces and torques for a test matrix that accounts for a range of spindle feeds, are used to determine axial pressures and energy consumptions. Two methods are used to determine the energy consumption and a cost analysis is developed. The cost analysis presented indicates that the energy consumption of RFW is one-tenth that of fusion butt welding. Thus, reduced environmental impacts and immense cost savings can be realized with a shift in style of welding operations from fusion butt welding to RFW.

REFERENCES

[1] Acare4europe.org. (2018). *About ACARE | Acare*. [online] Available at: http://www.acare4europe.org/about-acare [Accessed 1 Apr. 2018].
[2] Amanat, N., James, N. and McKenzie, D. (2010). Welding methods for joining thermoplastic polymers for the hermetic enclosure of medical devices. *Medical Engineering & Physics*, 32(7), pp.690-699.
[3] Takasu, N. (2003). Friction welding of plastics. *Welding International*, 17(11), pp.856-859.
[4] Haykalplast.com. (2018). [online] Available at: http://www.haykalplast.com/downloads/catalogs/HaykalPlast-PeProductCatalog.pdf [Accessed 1 Feb. 2018].
[5] Troughton, M. (2008). *Handbook of plastics joining*. Norwich, NY: William Andrew Inc., pp.29-34.
[6] Shrivastava, A., Krones, M. and Pfefferkorn, F. (2015). Comparison of energy consumption and environmental impact of friction stir welding and gas metal arc welding for aluminum. *CIRP Journal of Manufacturing Science and Technology*, 9, pp.159-168.
[7] Crawford, R. and Tam, Y. (1981). Friction welding of plastics. *Journal of Materials Science*, 16(12), pp.3275-3282.
[8] Tappe, P. and Potente, H. (1989). New results on the spin welding of plastics. *Polymer Engineering and Science*, 29(23), pp.1655-1660.
[9] Alves, E., Piorino Neto, F. and An, C. (2010). Welding of AA1050 Aluminum with AISI 304 stainless steel by rotary friction welding process. *Journal of Aerospace Technology and Management*, 2(3), pp.301-306.
[10] Ammouri, A. and Hamade, R. (2015). Toward an affordable automation scheme of friction stir processing. ASME 2015 International Mechanical Engineering Congress and Exposition IMECE2015, November 13-19, 2015, Houston, Texas. DOI: 10.1115/IMECE2015-53314.
[11] Plasticpipe.org. (2018). *R-Value and Thermal Conductivity of PEX and PE-RT TR-48/2014*. [online] Available at: https://plasticpipe.org/pdf/tr48-r-value-thermal-conductivity-pex-pe-rt.pdf [Accessed 20 Apr. 2018].
[12] Barber, P. and Atkinson, J. (1972). Some microstructural features of the welds in butt-welded polyethylene and polybutene-1 pipes. *Journal of Materials Science*, 7(10), pp.1131-1136.
[13] Ritmoamerica.com. (2018). *TP 125 - Heating Plates - Ritmo America*. [online] Available at: http://www.ritmoamerica.com/product_single.php?id=20# [Accessed 20 Apr. 2018].
[14] Cho, Y., Hartnett, J. and Rohsenow, W. (1998). *Handbook of Heat Transfer (3rd Edition)*. McGraw-Hill.